ARTICLE

Robust biweight M-estimator-based simultaneous prediction intervals with applications in laboratory medicine

Maria Vivian Fabiola N. Sibonga and Michael Daniel C. Lucagbo*

School of Statistics, University of the Philippines, Diliman, Quezon City 1101, Philippines

ABSTRACT

Reference intervals are among the most widely used tools in medical decision-making. Moreover, in diagnosing complex diseases based on multiple analytes, multivariate reference regions (MRRs) are indispensable. In such cases, MRRs are more appropriate than separate univariate reference intervals because the latter fail to account for the correlations among the analytes. The usual approach to construct MRRs is through an ellipsoidal reference region under multivariate normality. However, laboratory practitioners are reluctant to use ellipsoidal MRRs since such MRRs cannot detect component-wise outliers. To address this problem, this study proposes a methodology to construct rectangular MRRs by computing robust simultaneous prediction intervals through an approach that makes use of Tukey's biweight estimator. Designed for symmetric multivariate distributions, the proposed procedure relaxes the multivariate normality assumption, which is a common assumption in computing reference regions. This study makes use of a nonparametric bootstrap solution to estimate a common prediction factor. The performance of the proposed procedure is evaluated through coverage probabilities and compared against a benchmark methodology. The results indicate that the proposed methodology shows consistently accurate performance regardless of the underlying data distribution, which suggests that it may be applied to data coming from any symmetric distribution.

INTRODUCTION

Background

Laboratory professionals measure and analyze health indicators such as a patient's cholesterol profile, glucose level, gout screen, and kidney function through the results of laboratory tests. To determine whether a result is consistent with a healthy reference population, laboratories use reference intervals, also known as reference ranges. The reference interval is obtained by taking the central 95% of measurements of the healthy population or reference population. Thus, the endpoints of a reference interval are the 2.5th and 97.5th percentiles of the reference population. If only an upper limit is required, we look for the 95th percentile; and if only a lower limit is required, we take the 5th percentile.

When diagnosing complex clinical conditions such as liver function, multiple analytes are needed to diagnose a patient accurately. Laboratory test results on these analytes are often correlated. Thus, the practice of using separate univariate reference intervals (i.e., one for each analyte) to diagnose the condition is not statistically sound because it fails to take into consideration the cross-correlations among the analytes. Such a scheme typically leads to an increase in the number of false positives. Rather, one should use a multivariate reference region (MRR), whose associated coverage probability attains the 95% nominal level. Whereas univariate reference intervals are estimated independently of each other, an MRR is estimated in a way that accounts for the cross-correlations among multiple analytes.

The conventional approach for constructing MRRs, especially when the data follow a multivariate normal distribution, is to construct ellipsoidal reference regions. While many modern statistical methods and data analyses are largely understood through elliptical geometry (Friendly et al. 2013), Wellek (2011) asserts that ellipsoidal regions are not ideal to use as MRRs because an ellipsoidal region cannot detect component-wise outliers. In other words, a patient who has been diagnosed as positive for a certain disease does not have information on which specific analytes caused the positive result. Moreover, ellipsoidal regions are difficult to interpret. To avoid this drawback of ellipsoidal regions, a natural alternative is to use rectangular MRRs. The first successful attempt at constructing rectangular MRRs is that of Wellek (2011), whose solution involves defining a region that is a function of unknown parameters and plugs in the estimates of these parameters. However, this only gives a point estimate of the rectangular reference region.

Lucagbo et al. (2022) developed a rectangular MRR with good coverage properties using a 95% prediction region criterion. Their study makes use of a parametric bootstrap under multivariate normality. While normality is a common distributional assumption in the laboratory medicine literature, most analyte measurements

*Corresponding author
Email Address: **mclucagbo@up.edu.ph**
Date received: 28 March 2026
Date revised: 11 May 2026
Date accepted: 22 May 2026
DOI: https://doi.org/10.54645/2026191PNA-71

KEYWORDS

Robust; Biweight; M-Estimator; Laboratory medicine; Multivariate Reference Region; Nonparametric bootstrap

do not in fact follow a normal distribution and therefore need to be transformed first to approximate normality (Horn and Pesce 2003; Ichihara and Boyd 2010). Applying normal distribution-based methods to non-normal data without preliminary transformation of the data can lead to invalid reference intervals. Another difficulty with data on analyte measurements is the preponderance of outliers. For these reasons, a robust method that depends little on the underlying data distribution and is resistant to the influence of outliers offers an ideal alternative approach to compute reference intervals.

Horn (1988) proposes a procedure to compute a prediction interval through a robust approach involving biweight estimators for location and scale parameters. It is applicable to any symmetric distribution (i.e., does not assume normality) and is resistant to the presence of outliers in the dataset. This approach has also been recommended by the Clinical and Laboratory Standards Institute (CLSI), as highlighted in its EP28-A3c guideline, in computing reference intervals (CLSI 2010). Nonetheless, the methodology of Horn (1988) only applies to the univariate case and thus cannot be extended directly to MRRs. This study takes up the multivariate case by proposing a methodology to compute robust simultaneous prediction intervals to be used as rectangular MRRs that possess robust properties.

Robust Statistics

Classical measures of location and scale like the mean and standard deviation are typically not robust. Both have a breakdown value of zero, and an unbounded influence function. On the other hand, the median and the median absolute deviation (MAD) are robust measures, each having a breakdown value of 0.50. Nonetheless, the median is less efficient because it has a large standard error under normality. An M-measure of location should balance the concerns regarding robustness and efficiency (Rousseeuw and Hubert 2018). See also Sections 2.2.4, 2.3, and 2.4 of Wilcox (2012) for further discussion. M-measures of location are classes of functions that determine μ_m, such that:

$$E\left[\psi\left(\frac{X-\mu_m}{\tau}\right)\right]=0 \qquad (1.2.1)$$

where τ is a measure of scale and ψ is an odd function. An ideal choice for τ is the MAD because of its high breakdown value. Suppose the data consist of the univariate random sample $X_1, X_2, \ldots, X_n$. The estimator for, μ_m given by $\hat{\mu}_m$, is computed such that:

$$\sum_{i=1}^{n}\psi\left(\frac{X_i-\hat{\mu}_m}{\tau}\right)=0. \qquad (1.2.2)$$

Not all M-estimators of location meet the desired properties. An important attribute to consider is that the appropriate ψ should give less weight to observations that are far from the middle part of the data and put no weight on the extremes. An M-estimator of location such as Tukey's biweight M-estimator is a popular choice. Tukey's biweight estimator is an example of a redescending M-estimator, which is an M-estimator whose ψ-functions are restricted to be nondecreasing near the origin, but decreasing toward 0 when far from the origin. The biweight estimator T_{bi} which has been shown to perform well under symmetric stretched-tail distributions (see, for instance, Kafadar (1982)), is obtained through the following choice of ψ in (1.2.2):

$$\psi(u)=\begin{cases}u(1-u^2)^2, & |u|<1\\ 0, & \text{otherwise.}\end{cases} \qquad (1.2.3)$$

Given the weight function:

$$w(u)=\begin{cases}(1-u^2)^2, & |u|<1\\ 0, & otherwise\end{cases} \qquad (1.2.4)$$

the value of T_{bi} is computed through iteration (described in detail in the next subsection) as a reweighted average of the observations:

$$T_{bi}=\frac{\sum_{i=1}^{n}X_i * w\left(\frac{X_i-T_{bi}}{c*s}\right)}{\sum_{i=1}^{n}w\left(\frac{X_i-T_{bi}}{c*s}\right)}, \qquad (1.2.5)$$

where c is a tuning constant and s is an estimate of scale. The weight function assigns zero weight to any observation outside the interval $(T_{bi}-cs, T_{bi}+cs)$. A weighted iterative calculation of T_{bi} is a more stable and encouraging solution for (1.2.2). The iterative calculation procedures based on (1.2.5) are explained in Subsection 1.3.

Biweight estimator and its variance estimator

In this subsection, we describe the iterative process to compute Tukey's biweight estimator T_{bi}. We use the notation $\text{med}\{X_1, X_2, \ldots, X_n\}$ to denote that sample median of the observations $X_1, X_2, \ldots, X_n$. The first form of s is the rescaled MAD, which we denote as s_{madn}. The formula for s_{madn} is given by:

$$s_{madn}=\frac{1}{z_{0.75}} * \text{med}\{|X_1-\text{med}\{X_1\ldots,X_n\}|,\ldots,|X_n-\text{med}\{X_1,\ldots,X_n\}|\} \qquad (1.3.1)$$

where $z_{0.75}$ is the 75th percentile of the standard normal distribution. Note that in obtaining s_{madn}, the value $z_{0.75}$ is used to rescale the MAD so that s_{madn} is a consistent estimator of the population standard deviation in the Gaussian case. The second form of the scale s is the biweight scale estimate s_{bi}, based on the theoretical asymptotic variance of T_{bi}:

$$s_{bi}=c*\tilde{s}\sqrt{\frac{n\sum_{i=1}^{n}\psi^2\left(\frac{X_i-T_{bi}^0}{c*\tilde{s}}\right)}{\left[\sum_{i=1}^{n}\psi'\left(\frac{X_i-T_{bi}^0}{c*\tilde{s}}\right)\right]*\max\left\{1,-1+\sum_{i=1}^{n}\psi'\left(\frac{X_i-T_{bi}^0}{c*\tilde{s}}\right)\right\}}} \qquad (1.3.2)$$

where:

$$\psi^2(u)=u^2(1-u^2)^4$$
$$\psi'(u)=(1-u^2)(1-5u^2),$$

the quantity T_{bi}^0 denotes the median of the sample, and $\tilde{s}$ may be taken to be s_{madn}. We note that s_{bi} is a robust estimate of scale that does more than twice as well as s_{madn} (Mosteller and Tukey, 1977). We shall now describe the iterative procedure needed to compute T_{bi}. Let T_{bi}^h be the value of T_{bi} at iteration h.

1. Starting at $h=0$, T_{bi}^h is the median:

$$T_{bi}^h=T_{bi}^0=\text{med}\{X_1,X_2,\ldots,X_n\}$$

Compute MAD s_{mad} and s_{madn}:

$$s_{mad}=\text{med}\left\{\left|X_1-T_{bi}^0\right|,\left|X_2-T_{bi}^0\right|,\ldots,\left|X_n-T_{bi}^0\right|\right\}$$
$$s_{madn}=\frac{1}{z_{0.75}} * s_{mad}.$$

2. Compute T_{bi}^h for the next iterations through:

$$T_{bi}^{h+1}=\frac{\sum_{i=1}^{n}X_i * w\left(\frac{X_i-T_{bi}^h}{c*s_{madn}}\right)}{\sum_{i=1}^{n}w\left(\frac{X_i-T_{bi}^h}{c*s_{madn}}\right)} \quad h=0,1,2,\ldots$$

3. Stop the iteration when the relative change between the previous and current T_{bi} is less than 0.001%.

4. Take T_{bi} from the last iteration as the final biweight estimate of location.

Kafadar (1982) defines the finite-sample approximation to the variance of T_{bi} based on the biweight scale estimate s_{bi} as:

$$S_T^2 = (c * s_{bi})^2 * \frac{\sum_{i=1}^{n} \psi^2\left(\frac{X_i - T_{bi}}{c * s_{bi}}\right)}{\left[\sum_{i=1}^{n} \psi'\left(\frac{X_i - T_{bi}}{c * s_{bi}}\right)\right] * \max\left\{1, -1 + \sum_{i=1}^{n} \psi'\left(\frac{X_i - T_{bi}}{c * s_{bi}}\right)\right\}}, \quad (1.3.3)$$

where c is a tuning constant. The T_{bi} value used in (1.3.3) is the final biweight estimate of location. The estimator S_T^2 used by Kafadar (1982) is simply an estimator of the variance of T_{bi}, which may be obtained from the more general theoretical asymptotic variance of an M-estimate derived by Huber (1981). No claim is made about whether it is a robust estimator of the variance.

Biweight prediction interval

The robust prediction interval proposed by Horn (1988), which is based on the robust biweight M-estimator of location and scale, takes the form in (1.3.4). It assumes only that the data come from a symmetric population that is "Gaussian in the middle" (Horn, 1988). Due to its robust properties, it is not dependent on distributional assumptions. The prediction factor k in (1.3.4) may be taken as the $100\left(\frac{1+\gamma}{2}\right)$ th percentile of the Student's t-distribution with df $= n - 1$.

$$T_{bi} \pm k\left(S_T^2 + s_{bi}^2\right)^{\frac{1}{2}}. \quad (1.3.4)$$

Multivariate symmetric distributions

The methodologies proposed in this study are intended to be applicable to any symmetric multivariate distribution. We shall present three different definitions of symmetry for multivariate distributions, namely, radial, angular, and elliptical symmetry. Let $\boldsymbol{X}$ be a $p \times 1$ continuous random vector with PDF $f(\boldsymbol{x})$. Let $\boldsymbol{c} \in \mathbb{R}^p$ be a constant vector. Radial symmetry about $\boldsymbol{c}$ is satisfied if $\boldsymbol{X} - \boldsymbol{c} \overset{d}{=} -(\boldsymbol{X} - \boldsymbol{c})$, where $\overset{d}{=}$ denotes equality in distribution. Moreover, $\boldsymbol{X}$ is angularly symmetric about $\boldsymbol{c}$ if $\frac{\boldsymbol{X}-\boldsymbol{c}}{\|\boldsymbol{X}-\boldsymbol{c}\|} \overset{d}{=} -\frac{\boldsymbol{X}-\boldsymbol{c}}{\|\boldsymbol{X}-\boldsymbol{c}\|}$ where $\|\cdot\|$ denotes the L^2 norm. Finally, $\boldsymbol{X}$ is elliptically symmetric if for some vector $\boldsymbol{\mu}$ and positive semidefinite matrix $\boldsymbol{\Sigma}$, and some scalar function ψ, we have $\phi_{\boldsymbol{X}-\boldsymbol{\mu}}(\boldsymbol{t}) = \psi(\boldsymbol{t}'\boldsymbol{\Sigma}\boldsymbol{t})$, where ϕ is the characteristic function of $\boldsymbol{X}$. See also Fisz (1989), Liu (1988), and Cambanis et al. (1981) for the definitions of radial, angular, and elliptical symmetry, respectively. Elliptically symmetric distributions are radially and angularly symmetric in general. Examples of elliptically symmetric distributions include the multivariate normal, multivariate Cauchy, and multivariate t distributions. Table 1.1 shows their respective density functions. See also Fang et al. (1990) for a book-length discussion of symmetric multivariate distributions.

Table 1.1: Some multivariate distributions and their density functions

Distribution	PDF	Location parameter	Scale parameter
Multivariate normal	$f(\boldsymbol{x};\boldsymbol{\mu},\boldsymbol{\Sigma}) = (2\pi)^{-\frac{p}{2}}\lvert\boldsymbol{\Sigma}\rvert^{-\frac{1}{2}}\exp\left(-\frac{1}{2}(\boldsymbol{x}-\boldsymbol{\mu})'\boldsymbol{\Sigma}^{-1}(\boldsymbol{x}-\boldsymbol{\mu})\right)$	$\boldsymbol{\mu} = p \times 1$ vector	$\boldsymbol{\Sigma} = p \times p$ positive define matrix
Multivariate Cauchy	$f(\boldsymbol{x};\boldsymbol{\mu},\boldsymbol{\Sigma}) = \frac{\pi^{-p/2}\lvert\boldsymbol{\Sigma}\rvert^{-\frac{1}{2}}\Gamma\left(\frac{1+p}{2}\right)}{\Gamma\left(\frac{1}{2}\right)[1+(\boldsymbol{x}-\boldsymbol{\mu})'\boldsymbol{\Sigma}^{-1}(\boldsymbol{x}-\boldsymbol{\mu})]^{(1+p)/2}}$		
Multivariate t with ν degrees of freedom (df)	$f(\boldsymbol{x};\boldsymbol{\mu},\boldsymbol{\Sigma},\nu) = \frac{\nu^{-p/2}\pi^{-p/2}\lvert\boldsymbol{\Sigma}\rvert^{-\frac{1}{2}}\Gamma\left(\frac{\nu+p}{2}\right)}{\Gamma\left(\frac{\nu}{2}\right)\left[1+\frac{1}{\nu}(\boldsymbol{x}-\boldsymbol{\mu})'\boldsymbol{\Sigma}^{-1}(\boldsymbol{x}-\boldsymbol{\mu})\right]^{(\nu+p)/2}}$		
Multivariate Logistic	$f(\boldsymbol{x};\boldsymbol{\mu},\boldsymbol{\beta}) = \frac{p!\exp\left(-\sum_{j=1}^{p}\frac{x_j-\mu_j}{\beta_j}\right)}{\left[\prod_{j=1}^{p}\beta_j\right]\left[1+\sum_{j=1}^{p}\exp\left(-\frac{x_j-\mu_j}{\beta_j}\right)\right]^{1+p}}$, $\boldsymbol{x} = \begin{bmatrix}x_1\\ \vdots \\ x_p\end{bmatrix}$	$\boldsymbol{\mu} = \begin{bmatrix}\mu_1\\ \vdots \\ \mu_p\end{bmatrix}$	$\boldsymbol{\beta} = \begin{bmatrix}\beta_1\\ \vdots \\ \beta_p\end{bmatrix}$

MATERIALS AND METHODS

We shall now discuss the proposed methodology to obtain the rectangular MRR. This study derives two-sided simultaneous prediction intervals, as well as upper and lower one-sided simultaneous prediction intervals. An application to real-life data will also be presented. We start with developing the procedure to compute two-sided simultaneous prediction intervals that make use of the biweight method of Horn (1988). Let $\boldsymbol{X}_1, \boldsymbol{X}_2, \ldots, \boldsymbol{X}_n$ be the $p \times 1$ multivariate observations (representing the multivariate measurements from subjects), assumed to be a random sample from some symmetric multivariate distribution $f(\boldsymbol{x};\boldsymbol{\theta})$ indexed by $\boldsymbol{\theta}$. Define $\boldsymbol{X} = (X_1, X_2, \ldots, X_p)'$ to be a future observation from $f(\boldsymbol{x};\boldsymbol{\theta})$ that is independent of the random sample. Suppose it is of interest to compute simultaneous prediction intervals for the components of $\boldsymbol{X}$ and suppose that the quantities $T_{bi(j)}$ $s_{bi(j)}^2$, and $S_{T(j)}^2$ are as presented in Sections 1.2 and 1.3 but computed from the jth components of $\boldsymbol{X}_1, \boldsymbol{X}_2, \ldots, \boldsymbol{X}_n$. The simultaneous prediction intervals are of the following form:

$$T_{bi(j)} \pm \kappa\sqrt{s_{bi(j)}^2 + S_{T(j)}^2}, j = 1, 2, \ldots, p, \quad (2.1.1)$$

where the factor κ is an unknown prediction factor that depends on the cross-correlations of the components of $\boldsymbol{X}$. We estimate κ subject to the criterion for simultaneous prediction intervals, described in (2.1.2). By rewriting (2.1.2) as in (2.1.4), we express κ as a quantile and estimate it through a nonparametric bootstrap procedure, which consists of sampling from the empirical CDF of $\boldsymbol{X}_1, \boldsymbol{X}_2, \ldots, \boldsymbol{X}_n$. Since the data consist of independent and identically distributed random vectors by assumption, then by the Glivenko-Cantelli Theorem, their empirical CDF converges uniformly to the true CDF of the multivariate observations (Glivenko, 1933). See also Davison and Hinkley (1997) for the theoretical conditions on the consistency of the bootstrap. Equation (2.1.4) gives us a basis for the bootstrap procedure.

$$P\left(X_j \in T_{bi(j)} \pm \kappa\sqrt{s^2_{bi(j)} + S^2_{T(j)}}, \forall\, j = 1, 2, \ldots, p\right) = 1 - \alpha \quad (2.1.2)$$

$$\Leftrightarrow P\left(-\kappa \le \frac{X_j - T_{bi(j)}}{\sqrt{s^2_{bi(j)} + S^2_{T(j)}}} \le \kappa, \forall\, j = 1, 2, \ldots, p\right) = 1 - \alpha \quad (2.1.3)$$

$$\Leftrightarrow P\left(\max_{1\le j\le p}\left|\frac{X_j - T_{bi(j)}}{\sqrt{s^2_{bi(j)} + S^2_{T(j)}}}\right| \le \kappa\right) = 1 - \alpha. \quad (2.1.4)$$

When only upper reference limits are required, we compute upper one-sided simultaneous prediction limits, through the criterion in (2.1.5), which is also equivalent to (2.1.6). Equation (2.1.6) expresses κ as a quantile and may be used as basis for a nonparametric bootstrap procedure to estimate κ.

$$P\left(X_j \le T_{bi(j)} + \kappa\sqrt{s^2_{bi(j)} + S^2_{T(j)}}, \forall\, j = 1, 2, \ldots, p\right) = 1 - \alpha \quad (2.1.5)$$

$$\Leftrightarrow P\left(\max_{1\le j\le p}\frac{X_j - T_{bi(j)_j}}{\sqrt{s^2_{bi(j)} + S^2_{T(j)}}} \le \kappa\right) = 1 - \alpha. \quad (2.1.6)$$

Finally, to compute lower one-sided simultaneous prediction limits, we use the criterion in (2.1.7) or (2.1.8), which once again expresses κ as a quantile and sets the stage for a nonparametric bootstrap solution for κ.

$$P\left(T_{bi(j)} + \kappa\sqrt{s^2_{bi(j)} + S^2_{T(j)}} \le X_j, \forall\, j = 1, 2, \ldots, p\right) = 1 - \alpha \quad (2.1.7)$$

$$\Leftrightarrow P\left(\min_{1\le j\le p}\frac{X_j - T_{bi(j)}}{\sqrt{s^2_{bi(j)} + S^2_{T(j)}}} < \kappa\right) = \alpha. \quad (2.1.8)$$

In (2.1.1) to (2.1.8) we have used a common prediction factor κ. Technically, this can only be justified if the marginal distributions of the "studentized" quantities in (2.1.3) are identical. However, this will not be the case unless restrictive assumptions are made on the scale parameter matrix. On the other hand, it seems necessary to use a common prediction factor, because the problem becomes numerically intractable if this is not assumed.

Algorithm 1 presents the proposed procedure to compute the simultaneous prediction intervals. The implementation of Algorithm 1 involves the use of tuning constants c_1 and c_2. We use $c_1 = 3.7$ to derive T_{bi} and S^2_T, as recommended by Horn (1988). As for c_2, which is used in computing s^2_{bi}, a much larger value must be considered since substantial information about the scale lies in the tails. This study uses $c_2 = 205.6$. The values of c_1 and c_2 used in this study are also the ones that appear in the CLSI (2010) illustration of the robust method. To evaluate the performance of the proposed methodology, we compute the estimated coverage probabilities. Algorithm 2 describes the procedure to compute estimated coverage probabilities.

Algorithm 1. Proposed procedure to compute the robust two-sided and one-sided simultaneous prediction intervals to be used in forming the MRR

Suppose the dataset consists of the $p \times 1$ vectors $\boldsymbol{X}_1, \boldsymbol{X}_2, \ldots, \boldsymbol{X}_n$ from the continuous symmetric distribution $f(\boldsymbol{x}; \boldsymbol{\theta})$ and write $\boldsymbol{X}_i = \left(X_{i1}, X_{i2}, \ldots, X_{ip}\right)'$.

Step 1:

For each $j = 1, 2, \ldots, p$:

a. Compute the biweight estimate of location $T_{bi(j)}$ as follows:

1. At $h = 0$, set the initial estimate of $T_{bi(j)}$ as the median:
$$T^h_{bi(j)} = T^0_{bi(j)} = \text{med}\{X_{1j}, X_{2j}, \ldots, X_{nj}\}.$$
2. Compute $s_{mad(j)}$ as the median absolute deviation (MAD):
$$s_{mad(j)} = \text{med}\left\{\left|X_{1j} - T^0_{bi(j)}\right|, \left|X_{2j} - T^0_{bi(j)}\right|, \ldots, \left|X_{nj} - T^0_{bi(j)}\right|\right\}.$$
3. Compute the rescaled MAD:
$$s_{madn(j)} = \frac{1}{z_{0.75}} * s_{mad(j)}.$$
4. Compute $T^h_{bi(j)}$ for the next iterations:
$$T^{h+1}_{bi(j)} = \frac{\sum_{i=1}^n X_{ij} * w\left(\frac{X_{ij} - T^h_{bi(j)}}{c_1 * s_{madn(j)}}\right)}{\sum_{i=1}^n w\left(\frac{X_{ij} - T^h_{bi(j)}}{c_1 * s_{madn(j)}}\right)} \quad h = 0, 1, 2, \ldots,$$
where $c_1 = 3.7$ and $w(\cdot)$ is the weight function defined in (1.2.4).
5. Stop the iteration when the relative change between the previous and current $T_{bi(j)}$ is less than 0.001%.
6. The final value of $T_{bi(j)}$ represents the biweight estimate of location.

b. Compute the biweight estimates of scale as follows:

1. Compute $s_{bi[c_2](j)}$ using tuning constant $c_2 = 205.6$
$$s_{bi[c_2](j)} = c_2 * s_{madn(j)} \sqrt{\frac{n\sum_{i=1}^n \psi^2\left(\frac{X_{ij} - T^0_{bi(j)}}{c_2 * s_{madn(j)}}\right)}{\left[\sum_{i=1}^n \psi'\left(\frac{X_{ij} - T^0_{bi(j)}}{c_2 * s_{madn(j)}}\right)\right] * \max\left\{1, -1 + \sum_{i=1}^n \psi'\left(\frac{X_{ij} - T^0_{bi(j)}}{c_2 * s_{madn(j)}}\right)\right\}}}.$$

2. Compute $s_{bi[c_1](j)}$ and $S_{T[c_1](j)}$ using tuning constant $c_1 = 3.7$

$$s_{bi[c_1](j)} = c_1 * s_{madn(j)} \sqrt{\frac{n\sum_{i=1}^{n}\psi^2\left(\frac{X_{ij}-T^0_{bi(j)}}{c_1 * s_{madn(j)}}\right)}{\left[\sum_{i=1}^{n}\psi'\left(\frac{X_{ij}-T^0_{bi(j)}}{c_1 * s_{madn(j)}}\right)\right] * \max\left\{1, -1+\sum_{i=1}^{n}\psi'\left(\frac{X_{ij}-T^0_{bi(j)}}{c_1 * s_{madn(j)}}\right)\right\}}}$$

$$S_{T[c_1](j)} = c_1 * s_{bi[c_1](j)} \sqrt{\frac{\sum_{i=1}^{n}\psi^2\left(\frac{X_{ij}-T_{bi(j)}}{c_1 * s_{bi[c_1](j)}}\right)}{\left[\sum_{i=1}^{n}\psi'\left(\frac{X_{ij}-T_{bi(j)}}{c_1 * s_{bi[c_1](j)}}\right)\right] * \max\left\{1, -1+\sum_{i=1}^{n}\psi'\left(\frac{X_{ij}-T_{bi(j)}}{c_1 * s_{bi[c_1](j)}}\right)\right\}}}.$$

Step 2:

a. Perform the nonparametric bootstrap. For each $b = 1, 2, \ldots, B$, do the following:

1. Sample $\boldsymbol{X}^*_{1b}, \boldsymbol{X}^*_{2b}, \ldots, \boldsymbol{X}^*_{nb}$ using SRSWR from $\{\boldsymbol{X}_1, \boldsymbol{X}_2, \ldots, \boldsymbol{X}_n\}$. Write the components of $\boldsymbol{X}^*_{ib}$ as $\boldsymbol{X}^*_{ib} = \left(X^*_{i1b}, X^*_{i2b}, \ldots, X^*_{ipb}\right)'$
2. For each $j = 1, 2, \ldots, p$, compute the biweight estimates of location and scale: $T^*_{bi(jb)}$, $s^*_{bi[c_2](jb)}$, and $S^*_{T[c_1](jb)}$ using the same procedures as $T_{bi(j)}$, $s_{bi[c_2](j)}$, and $S_{T[c_1](j)}$, respectively, but applied to the bth bootstrap sample.
3. Sample $\boldsymbol{X}^*_b$ from $\{\boldsymbol{X}_1, \boldsymbol{X}_2, \ldots, \boldsymbol{X}_n\}$ and write $\boldsymbol{X}^*_b = \left(X^*_{1b}, X^*_{2b}, \ldots, X^*_{pb}\right)'$.
4. Compute κ^*_b according to the type of simultaneous prediction intervals:

4a. Two-sided simultaneous prediction intervals

$$\kappa^*_b = \max_{1\le j\le p}\left|\frac{X^*_{jb} - T^*_{bi(jb)}}{\sqrt{s^{2*}_{bi[c_2](jb)} + S^{2*}_{T[c_1](jb)}}}\right|$$

4b. Upper one-sided simultaneous prediction intervals

$$\kappa^*_b = \max_{1\le j\le p}\frac{X^*_{jb} - T^*_{bi(jb)}}{\sqrt{s^{2*}_{bi[c_2](jb)} + S^{2*}_{T[c_1](jb)}}}$$

4c. Lower one-sided simultaneous prediction intervals

$$\kappa^*_b = \min_{1\le j\le p}\frac{X^*_{jb} - T^*_{bi(jb)}}{\sqrt{s^{2*}_{bi[c_2](jb)} + S^{2*}_{T[c_1](jb)}}}.$$

b. Compute the $\hat{\kappa}$ prediction factor according to the type of prediction intervals:

1. Two-sided simultaneous prediction intervals
   $\hat{\kappa} = (1-\alpha)$-quantile of $\{\kappa^*_1, \kappa^*_2, \ldots, \kappa^*_B\}$

2. Upper one-sided simultaneous prediction intervals
   $\hat{\kappa} = (1-\alpha)$-quantile of $\{\kappa^*_1, \kappa^*_2, \ldots, \kappa^*_B\}$

3. Lower one-sided simultaneous prediction intervals
   $\hat{\kappa} = \alpha$-quantile of $\{\kappa^*_1, \kappa^*_2, \ldots, \kappa^*_B\}$

Step 3:

The $(1-\alpha)100\%$ simultaneous prediction intervals are given by:

a. Two-sided simultaneous prediction intervals

$$\left[T_{bi(1)} \pm \hat{\kappa}\sqrt{s^2_{bi[c_2](1)} + S^2_{T[c_1](1)}}\right] \times \left[T_{bi(2)} \pm \hat{\kappa}\sqrt{s^2_{bi[c_2](2)} + S^2_{T[c_1](2)}}\right] \times \cdots \times \left[T_{bi(p)} \pm \hat{\kappa}\sqrt{s^2_{bi[c_2](p)} + S^2_{T[c_1](p)}}\right]$$

b. Upper one-sided simultaneous prediction intervals

$$\left(-\infty, T_{bi(1)} + \hat{\kappa}\sqrt{s^2_{bi[c_2](1)} + S^2_{T[c_1](1)}}\right] \times \left(-\infty, T_{bi(2)} + \hat{\kappa}\sqrt{s^2_{bi[c_2](2)} + S^2_{T[c_1](2)}}\right] \times \cdots \times \left(-\infty, T_{bi(p)} + \hat{\kappa}\sqrt{s^2_{bi[c_2](p)} + S^2_{T[c_1](p)}}\right]$$

c. Lower one-sided simultaneous prediction intervals

$$\left[T_{bi(1)} + \hat{\kappa}\sqrt{s^2_{bi[c_2](1)} + S^2_{T[c_1](1)}}, \infty\right) \times \left[T_{bi(2)} + \hat{\kappa}\sqrt{s^2_{bi[c_2](2)} + S^2_{T[c_1](2)}}, \infty\right) \times \cdots \times \left[T_{bi(p)} + \hat{\kappa}\sqrt{s^2_{bi[c_2](p)} + S^2_{T[c_1](p)}}, \infty\right).$$

Algorithm 2. Procedure to compute the estimated coverage probability associated with the proposed procedure to compute the robust simultaneous prediction intervals

Step 1:

a. Generate $\boldsymbol{X}_1, \boldsymbol{X}_2, \ldots, \boldsymbol{X}_n$ from the continuous symmetric distribution $f(\boldsymbol{x}; \boldsymbol{\theta})$.
b. Compute the simultaneous prediction intervals using Algorithm 1.

Step 2:

a. Generate $\boldsymbol{X} = \left(X_1, X_2, \ldots, X_p\right)'$ from $f(\boldsymbol{x}; \boldsymbol{\theta})$.
b. Evaluate the indicator function according to the type of simultaneous prediction intervals:

1. Two-sided simultaneous prediction intervals

$$I = \begin{cases} 1, & X_j \in T_{bi(j)} \pm \hat{\kappa}\sqrt{s^2_{bi[c_2](j)} + S^2_{T[c_1](j)}} \quad \forall\, j = 1, 2, \ldots, p \\ 0, & otherwise \end{cases}$$

2. Upper one-sided simultaneous prediction intervals

$$I = \begin{cases} 1, & X_j \leq T_{bi(j)} + \hat{\kappa}\sqrt{s^2_{bi[c_2](j)} + S^2_{T[c_1](j)}} \quad \forall\, j = 1, 2, \ldots, p \\ 0, & otherwise \end{cases}$$

3. Lower one-sided simultaneous prediction intervals

$$I = \begin{cases} 1, & X_j \geq T_{bi(j)} + \hat{\kappa}\sqrt{s^2_{bi[c_2](j)} + S^2_{T[c_1](j)}} \quad \forall\, j = 1, 2, \ldots, p \\ 0, & otherwise \end{cases}$$

Step 3:

Repeat Steps 1 to 2 up to 5000 times. After completion, compute the average result of the indicator function I, from Step 2b. This represents our estimate of the coverage probability.

RESULTS AND DISCUSSION

Simulation Results

As already mentioned, to evaluate the performance of the proposed methodology, we shall be estimating the coverage probability. Data will be generated from the (elliptically) symmetric multivariate distributions in Table 1.1, with dimensions $p = 2, 3$. The location parameters to be used are zero-vectors and the scale parameters to be used are Σ_1 to Σ_6, shown below. Three different sample sizes are used: 50, 100, and 200. Lastly, the nominal level is set at 0.95.

$$\boldsymbol{\Sigma}_1 = \begin{bmatrix} 1 & 0.5 \\ 0.5 & 1 \end{bmatrix}, \quad \boldsymbol{\Sigma}_2 = \begin{bmatrix} 1 & -0.4 \\ -0.4 & 1 \end{bmatrix}, \quad \boldsymbol{\Sigma}_3 = \begin{bmatrix} 1 & 0 \\ 0 & 1 \end{bmatrix}, \quad \boldsymbol{\Sigma}_4 = \begin{bmatrix} 1 & 0.5 & 0.5 \\ 0.5 & 1 & 0.5 \\ 0.5 & 0.5 & 1 \end{bmatrix},$$

$$\boldsymbol{\Sigma}_5 = \begin{bmatrix} 1 & -0.4 & -0.4 \\ -0.4 & 1 & -0.4 \\ -0.4 & -0.4 & 1 \end{bmatrix}, \quad \boldsymbol{\Sigma}_6 = \begin{bmatrix} 1 & -0.1 & -0.4 \\ -0.1 & 1 & 0.7 \\ -0.4 & 0.7 & 1 \end{bmatrix}, \quad \boldsymbol{\Sigma}_7 = \begin{bmatrix} 1 & 0 & 0 \\ 0 & 1 & 0 \\ 0 & 0 & 1 \end{bmatrix}.$$

The performance of the proposed methodology will be compared to the procedure of Lucagbo et al. (2022), which computes a prediction region through a parametric bootstrap solution under multivariate normality. The methodology of Lucagbo et al. (2022) will also be referred to as the "benchmark methodology." Table 3.1 presents the estimated coverage probabilities for the two-sided simultaneous prediction intervals and the estimated standard errors of the coverage probabilities. Under multivariate normality, the coverage probabilities associated with the proposed methodology and that of the benchmark methodology are comparable and are close to the nominal level. It is no surprise that the latter methodology shows accurate performance as it is designed primarily for the multivariate normal distribution. Nonetheless, the proposed methodology's performance is comparable to that of the benchmark. When the underlying distribution is heavy-tailed (i.e., the multivariate Cauchy and multivariate t distributions), we see differences in the performances of the two methodologies. The results corresponding to the multivariate Cauchy show that the proposed methodology still achieves accurate coverage probabilities across all scenarios. On the other hand, the benchmark methodology tends to show conservative performance (i.e., coverage probabilities over 0.95) for a sample size of $n = 200$. The results for the multivariate t distribution with df = 5 show the coverage probabilities associated with the benchmark methodology tend to be liberal (i.e., coverage probabilities under 0.95), while the proposed methodology remains accurate. For the multivariate t with df = 10, there is an improvement in the performance of the benchmark methodology (presumably because now the shape of the distribution approaches that of the multivariate normal), and the proposed methodology maintains its accurate coverage. The estimated standard errors of the coverage probabilities are shown in parentheses. Note that a confidence interval for the true coverage may be formed via the normal approximation formula $\hat{p} \pm$

$1.96 \times \text{se}(\hat{p})$, where $\hat{p}$ is the coverage probability and $\text{se}(\hat{p})$ denotes its estimated standard error.

Table 3.1: Estimated coverage probabilities (and their corresponding estimated standard errors expressed in parentheses) associated with the approaches to compute two-sided simultaneous prediction intervals using the (1) proposed methodology and (2) methodology of Lucagbo et al. (2022). The nominal level is set at 95%.

p	n	Location parameter	Scale parameter	Distribution							
				Multivariate normal		Multivariate Cauchy		Multivariate t with df = 5		Multivariate t with df = 10	
				(1)	(2)	(1)	(2)	(1)	(2)	(1)	(2)
2	50	$\begin{bmatrix}0\\0\end{bmatrix}$	$\boldsymbol{\Sigma}_1$	0.9492 (0.0031)	0.9486 (0.0031)	0.9502 (0.0031)	0.9428 (0.0033)	0.9440 (0.0033)	0.9368 (0.0034)	0.9450 (0.0032)	0.9424 (0.0033)
			$\boldsymbol{\Sigma}_2$	0.9496 (0.0031)	0.9486 (0.0031)	0.9520 (0.0030)	0.9424 (0.0033)	0.9474 (0.0032)	0.9320 (0.0036)	0.9436 (0.0033)	0.9328 (0.0035)
			$\boldsymbol{\Sigma}_3$	0.9500 (0.0031)	0.9528 (0.0030)	0.9516 (0.0030)	0.9402 (0.0034)	0.9516 (0.0030)	0.9312 (0.0036)	0.9444 (0.0032)	0.9366 (0.0034)
	100	$\begin{bmatrix}0\\0\end{bmatrix}$	$\boldsymbol{\Sigma}_1$	0.9514 (0.0030)	0.9550 (0.0029)	0.9520 (0.0030)	0.9600 (0.0028)	0.9468 (0.0032)	0.9330 (0.0035)	0.9516 (0.0030)	0.9418 (0.0033)
			$\boldsymbol{\Sigma}_2$	0.9458 (0.0032)	0.9474 (0.0032)	0.9518 (0.0030)	0.9576 (0.0028)	0.9486 (0.0031)	0.9392 (0.0034)	0.9518 (0.0030)	0.9418 (0.0033)
			$\boldsymbol{\Sigma}_3$	0.9480 (0.0031)	0.9482 (0.0031)	0.9518 (0.0030)	0.9594 (0.0028)	0.9436 (0.0033)	0.9306 (0.0036)	0.9496 (0.0031)	0.9382 (0.0034)
	200	$\begin{bmatrix}0\\0\end{bmatrix}$	$\boldsymbol{\Sigma}_1$	0.9452 (0.0032)	0.9456 (0.0032)	0.9526 (0.0030)	0.9672 (0.0025)	0.9500 (0.0031)	0.9376 (0.0034)	0.9474 (0.0032)	0.9440 (0.0033)
			$\boldsymbol{\Sigma}_2$	0.9450 (0.0032)	0.9530 (0.0030)	0.9456 (0.0032)	0.9722 (0.0023)	0.9476 (0.0032)	0.9374 (0.0034)	0.9558 (0.0029)	0.9414 (0.0033)
			$\boldsymbol{\Sigma}_3$	0.9516 (0.0030)	0.9448 (0.0032)	0.9440 (0.0033)	0.9724 (0.0023)	0.9432 (0.0033)	0.9354 (0.0035)	0.9492 (0.0031)	0.9428 (0.0033)
3	50	$\begin{bmatrix}0\\0\\0\end{bmatrix}$	$\boldsymbol{\Sigma}_4$	0.9472 (0.0032)	0.9526 (0.0030)	0.9540 (0.0030)	0.9380 (0.0034)	0.9440 (0.0033)	0.9224 (0.0038)	0.9522 (0.0030)	0.9310 (0.0036)
			$\boldsymbol{\Sigma}_5$	0.9472 (0.0032)	0.9394 (0.0034)	0.9480 (0.0031)	0.9412 (0.0033)	0.9440 (0.0033)	0.9276 (0.0037)	0.9458 (0.0032)	0.9300 (0.0036)
			$\boldsymbol{\Sigma}_6$	0.9460 (0.0032)	0.9464 (0.0032)	0.9450 (0.0032)	0.9368 (0.0034)	0.9496 (0.0031)	0.9296 (0.0036)	0.9442 (0.0032)	0.9346 (0.0035)
			$\boldsymbol{\Sigma}_7$	0.9378 (0.0034)	0.9514 (0.0030)	0.9522 (0.0030)	0.9348 (0.0035)	0.9484 (0.0031)	0.9190 (0.0039)	0.9470 (0.0032)	0.9282 (0.0037)
	100	$\begin{bmatrix}0\\0\\0\end{bmatrix}$	$\boldsymbol{\Sigma}_4$	0.9540 (0.0030)	0.9506 (0.0031)	0.9526 (0.0030)	0.9550 (0.0029)	0.9484 (0.0031)	0.9252 (0.0037)	0.9494 (0.0031)	0.9368 (0.0034)
			$\boldsymbol{\Sigma}_5$	0.9460 (0.0032)	0.9508 (0.0031)	0.9534 (0.0030)	0.9534 (0.0030)	0.9442 (0.0032)	0.9286 (0.0036)	0.9530 (0.0030)	0.9356 (0.0035)
			$\boldsymbol{\Sigma}_6$	0.9504 (0.0031)	0.9400 (0.0034)	0.9560 (0.0029)	0.9490 (0.0031)	0.9492 (0.0031)	0.9276 (0.0037)	0.9482 (0.0031)	0.9402 (0.0034)
			$\boldsymbol{\Sigma}_7$	0.9432 (0.0033)	0.9464 (0.0032)	0.9558 (0.0029)	0.9542 (0.0030)	0.9466 (0.0032)	0.9224 (0.0038)	0.9526 (0.0030)	0.9316 (0.0036)
	200	$\begin{bmatrix}0\\0\\0\end{bmatrix}$	$\boldsymbol{\Sigma}_4$	0.9550 (0.0029)	0.9514 (0.0030)	0.9534 (0.0030)	0.9642 (0.0026)	0.9476 (0.0032)	0.9316 (0.0036)	0.9460 (0.0032)	0.9370 (0.0034)
			$\boldsymbol{\Sigma}_5$	0.9476 (0.0032)	0.9486 (0.0031)	0.9536 (0.0030)	0.9674 (0.0025)	0.9472 (0.0032)	0.9304 (0.0036)	0.9422 (0.0033)	0.9346 (0.0035)
			$\boldsymbol{\Sigma}_6$	0.9464 (0.0032)	0.9520 (0.0030)	0.9550 (0.0029)	0.9730 (0.0023)	0.9472 (0.0032)	0.9324 (0.0036)	0.9430 (0.0033)	0.9368 (0.0034)
			$\boldsymbol{\Sigma}_7$	0.9458 (0.0032)	0.9484 (0.0031)	0.9540 (0.0030)	0.9634 (0.0027)	0.9474 (0.0032)	0.9266 (0.0037)	0.9464 (0.0032)	0.9362 (0.0035)

Tables 3.2 and 3.3 present the estimated coverage probabilities for the upper and lower one-sided simultaneous prediction intervals, respectively. As before, when the distribution is multivariate normal, both the proposed and benchmark methodologies perform well, yielding coverage probabilities that range between approximately 0.94 and 0.95. When the underlying distribution is heavy-tailed, the proposed methodology still shows accurate performance that is clearly superior to that of the benchmark methodology. The benchmark methodology tends to result in conservative coverage in the multivariate Cauchy settings. It shows slightly liberal performance in some settings under the multivariate t with df = 5. On the whole, it seems that the performance of the benchmark methodology is largely dependent on the underlying distribution of the data. In contrast, the proposed methodology's performance is consistently accurate, attaining the nominal level regardless of the underlying distribution.

Table 3.2: Estimated coverage probabilities (and their corresponding estimated standard errors expressed in parentheses) associated with the approaches to compute upper one-sided simultaneous prediction intervals using the (1) proposed methodology and (2) methodology of Lucagbo et al. (2022). The nominal level is set at 95%.

				Distribution							
				Multivariate normal		Multivariate Cauchy		Multivariate t with df = 5		Multivariate t with df = 10	
p	n	Location parameter	Scale parameter	(1)	(2)	(1)	(2)	(1)	(2)	(1)	(2)
2	50	$\begin{bmatrix}0\\0\end{bmatrix}$	$\boldsymbol{\Sigma}_1$	0.9430 (0.0033)	0.9418 (0.0033)	0.9566 (0.0029)	0.9642 (0.0026)	0.9486 (0.0031)	0.9458 (0.0032)	0.9494 (0.0031)	0.9454 (0.0032)
			$\boldsymbol{\Sigma}_2$	0.9480 (0.0031)	0.9440 (0.0033)	0.9572 (0.0029)	0.9590 (0.0028)	0.9412 (0.0033)	0.9460 (0.0032)	0.9472 (0.0032)	0.9384 (0.0034)
			$\boldsymbol{\Sigma}_3$	0.9440 (0.0033)	0.9480 (0.0031)	0.9538 (0.0030)	0.9588 (0.0028)	0.9480 (0.0031)	0.9432 (0.0033)	0.9422 (0.0033)	0.9478 (0.0031)
	100	$\begin{bmatrix}0\\0\end{bmatrix}$	$\boldsymbol{\Sigma}_1$	0.9504 (0.0031)	0.9582 (0.0028)	0.9576 (0.0028)	0.9764 (0.0021)	0.9502 (0.0031)	0.9426 (0.0033)	0.9402 (0.0034)	0.9454 (0.0032)
			$\boldsymbol{\Sigma}_2$	0.9470 (0.0032)	0.9516 (0.0030)	0.9560 (0.0029)	0.9716 (0.0023)	0.9458 (0.0032)	0.9448 (0.0032)	0.9488 (0.0031)	0.9484 (0.0031)
			$\boldsymbol{\Sigma}_3$	0.9510 (0.0031)	0.9490 (0.0031)	0.9540 (0.0030)	0.9700 (0.0024)	0.9492 (0.0031)	0.9474 (0.0032)	0.9490 (0.0031)	0.9464 (0.0032)
	200	$\begin{bmatrix}0\\0\end{bmatrix}$	$\boldsymbol{\Sigma}_1$	0.9410 (0.0033)	0.9442 (0.0032)	0.9532 (0.0030)	0.9798 (0.0020)	0.9462 (0.0032)	0.9440 (0.0033)	0.9530 (0.0030)	0.9490 (0.0031)
			$\boldsymbol{\Sigma}_2$	0.9444 (0.0032)	0.9512 (0.0030)	0.9504 (0.0031)	0.9796 (0.0020)	0.9492 (0.0031)	0.9466 (0.0032)	0.9508 (0.0031)	0.9432 (0.0033)
			$\boldsymbol{\Sigma}_3$	0.9506 (0.0031)	0.9544 (0.0030)	0.9480 (0.0031)	0.9784 (0.0021)	0.9490 (0.0031)	0.9464 (0.0032)	0.9490 (0.0031)	0.9446 (0.0032)
3	50	$\begin{bmatrix}0\\0\\0\end{bmatrix}$	$\boldsymbol{\Sigma}_4$	0.9440 (0.0033)	0.9526 (0.0030)	0.9552 (0.0029)	0.9622 (0.0027)	0.9504 (0.0031)	0.9358 (0.0035)	0.9476 (0.0032)	0.9460 (0.0032)
			$\boldsymbol{\Sigma}_5$	0.9460 (0.0032)	0.9510 (0.0031)	0.9554 (0.0029)	0.9470 (0.0032)	0.9490 (0.0031)	0.9332 (0.0035)	0.9468 (0.0032)	0.9448 (0.0032)
			$\boldsymbol{\Sigma}_6$	0.9504 (0.0031)	0.9514 (0.0030)	0.9576 (0.0028)	0.9578 (0.0028)	0.9502 (0.0031)	0.9422 (0.0033)	0.9410 (0.0033)	0.9446 (0.0032)
			$\boldsymbol{\Sigma}_7$	0.9396 (0.0034)	0.9474 (0.0032)	0.9540 (0.0030)	0.9486 (0.0031)	0.9478 (0.0031)	0.9330 (0.0035)	0.9400 (0.0034)	0.9418 (0.0033)
	100	$\begin{bmatrix}0\\0\\0\end{bmatrix}$	$\boldsymbol{\Sigma}_4$	0.9504 (0.0031)	0.9492 (0.0031)	0.9502 (0.0031)	0.9720 (0.0023)	0.9476 (0.0032)	0.9462 (0.0032)	0.9464 (0.0032)	0.9438 (0.0033)
			$\boldsymbol{\Sigma}_5$	0.9452 (0.0032)	0.9460 (0.0032)	0.9556 (0.0029)	0.9642 (0.0026)	0.9450 (0.0032)	0.9364 (0.0035)	0.9490 (0.0031)	0.9442 (0.0032)
			$\boldsymbol{\Sigma}_6$	0.9502 (0.0031)	0.9452 (0.0032)	0.9538 (0.0030)	0.9666 (0.0025)	0.9464 (0.0032)	0.9424 (0.0033)	0.9488 (0.0031)	0.9456 (0.0032)
			$\boldsymbol{\Sigma}_7$	0.9410 (0.0033)	0.9530 (0.0030)	0.9504 (0.0031)	0.9632 (0.0027)	0.9448 (0.0032)	0.9388 (0.0034)	0.9414 (0.0033)	0.9454 (0.0032)
	200	$\begin{bmatrix}0\\0\\0\end{bmatrix}$	$\boldsymbol{\Sigma}_4$	0.9490 (0.0031)	0.9530 (0.0030)	0.9464 (0.0032)	0.9788 (0.0020)	0.9430 (0.0033)	0.9426 (0.0033)	0.9474 (0.0032)	0.9470 (0.0032)
			$\boldsymbol{\Sigma}_5$	0.9524 (0.0030)	0.9548 (0.0029)	0.9502 (0.0031)	0.9752 (0.0022)	0.9508 (0.0031)	0.9336 (0.0035)	0.9406 (0.0033)	0.9432 (0.0033)
			$\boldsymbol{\Sigma}_6$	0.9478 (0.0031)	0.9538 (0.0030)	0.9524 (0.0030)	0.9780 (0.0021)	0.9530 (0.0030)	0.9498 (0.0031)	0.9472 (0.0032)	0.9444 (0.0032)
			$\boldsymbol{\Sigma}_7$	0.9422 (0.0033)	0.9510 (0.0031)	0.9546 (0.0029)	0.9752 (0.0022)	0.9516 (0.0030)	0.9372 (0.0034)	0.9502 (0.0031)	0.9442 (0.0032)

Table 3.3: Estimated coverage probabilities (and their corresponding estimated standard errors expressed in parentheses) associated with the approaches to compute lower one-sided simultaneous prediction intervals using the (1) proposed methodology and (2) methodology of Lucagbo et al. (2022). The nominal level is set at 95%.

				Distribution							
				Multivariate normal		Multivariate Cauchy		Multivariate t with df = 5		Multivariate t with df = 10	
p	n	Location Parameter	Scale Parameter	(1)	(2)	(1)	(2)	(1)	(2)	(1)	(2)
2	50	$\begin{bmatrix}0\\0\end{bmatrix}$	$\boldsymbol{\Sigma}_1$	0.9480 (0.0031)	0.9468 (0.0032)	0.9594 (0.0028)	0.9652 (0.0026)	0.9426 (0.0033)	0.9408 (0.0033)	0.9480 (0.0031)	0.9428 (0.0033)
			$\boldsymbol{\Sigma}_2$	0.9466 (0.0032)	0.9492 (0.0031)	0.9596 (0.0028)	0.9590 (0.0028)	0.9416 (0.0033)	0.9460 (0.0032)	0.9460 (0.0032)	0.9462 (0.0032)
			$\boldsymbol{\Sigma}_3$	0.9480 (0.0031)	0.9496 (0.0031)	0.9520 (0.0030)	0.9650 (0.0026)	0.9466 (0.0032)	0.9480 (0.0031)	0.9520 (0.0030)	0.9456 (0.0032)
	100	$\begin{bmatrix}0\\0\end{bmatrix}$	$\boldsymbol{\Sigma}_1$	0.9472 (0.0032)	0.9486 (0.0031)	0.9534 (0.0030)	0.9714 (0.0024)	0.9488 (0.0031)	0.9480 (0.0031)	0.9436 (0.0033)	0.9444 (0.0032)
			$\boldsymbol{\Sigma}_2$	0.9456 (0.0032)	0.9488 (0.0031)	0.9546 (0.0029)	0.9696 (0.0024)	0.9422 (0.0033)	0.9404 (0.0033)	0.9442 (0.0032)	0.9420 (0.0033)
			$\boldsymbol{\Sigma}_3$	0.9412 (0.0033)	0.9512 (0.0030)	0.9562 (0.0029)	0.9724 (0.0023)	0.9458 (0.0032)	0.9476 (0.0032)	0.9478 (0.0031)	0.9482 (0.0031)

	200	$\begin{bmatrix}0\\0\end{bmatrix}$	$\boldsymbol{\Sigma}_1$	0.9492 (0.0031)	0.9458 (0.0032)	0.9528 (0.0030)	0.9852 (0.0017)	0.9508 (0.0031)	0.9500 (0.0031)	0.9530 (0.0030)	0.9490 (0.0031)
			$\boldsymbol{\Sigma}_2$	0.9496 (0.0031)	0.9480 (0.0031)	0.9502 (0.0031)	0.9772 (0.0021)	0.9480 (0.0031)	0.9446 (0.0032)	0.9534 (0.0030)	0.9466 (0.0032)
			$\boldsymbol{\Sigma}_3$	0.9516 (0.0030)	0.9476 (0.0032)	0.9492 (0.0031)	0.9782 (0.0021)	0.9544 (0.0030)	0.9508 (0.0031)	0.9502 (0.0031)	0.9438 (0.0033)
3	50	$\begin{bmatrix}0\\0\\0\end{bmatrix}$	$\boldsymbol{\Sigma}_4$	0.9518 (0.0030)	0.9546 (0.0029)	0.9536 (0.0030)	0.9550 (0.0029)	0.9458 (0.0032)	0.9468 (0.0032)	0.9502 (0.0031)	0.9414 (0.0033)
			$\boldsymbol{\Sigma}_5$	0.9420 (0.0033)	0.9512 (0.0030)	0.9532 (0.0030)	0.9436 (0.0033)	0.9496 (0.0031)	0.9342 (0.0035)	0.9422 (0.0033)	0.9374 (0.0034)
			$\boldsymbol{\Sigma}_6$	0.9506 (0.0031)	0.9488 (0.0031)	0.9584 (0.0028)	0.9518 (0.0030)	0.9450 (0.0032)	0.9440 (0.0033)	0.9438 (0.0033)	0.9490 (0.0031)
			$\boldsymbol{\Sigma}_7$	0.9474 (0.0032)	0.9454 (0.0032)	0.9536 (0.0030)	0.9568 (0.0029)	0.9524 (0.0030)	0.9356 (0.0035)	0.9490 (0.0031)	0.9412 (0.0033)
	100	$\begin{bmatrix}0\\0\\0\end{bmatrix}$	$\boldsymbol{\Sigma}_4$	0.9430 (0.0033)	0.9504 (0.0031)	0.9554 (0.0029)	0.9716 (0.0023)	0.9452 (0.0032)	0.9490 (0.0031)	0.9454 (0.0032)	0.9480 (0.0031)
			$\boldsymbol{\Sigma}_5$	0.9420 (0.0033)	0.9444 (0.0032)	0.9554 (0.0029)	0.9624 (0.0027)	0.9486 (0.0031)	0.9356 (0.0035)	0.9484 (0.0031)	0.9402 (0.0034)
			$\boldsymbol{\Sigma}_6$	0.9504 (0.0031)	0.9492 (0.0031)	0.9528 (0.0030)	0.9654 (0.0026)	0.9472 (0.0032)	0.9384 (0.0034)	0.9498 (0.0031)	0.9426 (0.0033)
			$\boldsymbol{\Sigma}_7$	0.9478 (0.0031)	0.9466 (0.0032)	0.9548 (0.0029)	0.9636 (0.0026)	0.9460 (0.0032)	0.9370 (0.0034)	0.9412 (0.0033)	0.9478 (0.0031)
	200	$\begin{bmatrix}0\\0\\0\end{bmatrix}$	$\boldsymbol{\Sigma}_4$	0.9468 (0.0032)	0.9498 (0.0031)	0.9500 (0.0031)	0.9836 (0.0018)	0.9552 (0.0029)	0.9492 (0.0031)	0.9484 (0.0031)	0.9500 (0.0031)
			$\boldsymbol{\Sigma}_5$	0.9430 (0.0033)	0.9458 (0.0032)	0.9516 (0.0030)	0.9742 (0.0022)	0.9508 (0.0031)	0.9354 (0.0035)	0.9436 (0.0033)	0.9394 (0.0034)
			$\boldsymbol{\Sigma}_6$	0.9492 (0.0031)	0.9448 (0.0032)	0.9546 (0.0029)	0.9768 (0.0021)	0.9468 (0.0032)	0.9474 (0.0032)	0.9498 (0.0031)	0.9428 (0.0033)
			$\boldsymbol{\Sigma}_7$	0.9488 (0.0031)	0.9510 (0.0031)	0.9516 (0.0030)	0.9770 (0.0021)	0.9480 (0.0031)	0.9440 (0.0033)	0.9486 (0.0031)	0.9390 (0.0034)

We also show some limited simulation results when the dimension is large ($p = 10$). For such simulations, we use the covariance matrices $\boldsymbol{\Sigma}_8 = 0.5\boldsymbol{I}_{10}, +0.5\mathbf{1}_{10}\mathbf{1}'_{10}$, which is a correlation matrix of exchangeable structure, with common correlation of $\rho = 0.5$. Although the dimension $p = 10$ is perhaps not too applicable in the context of reference regions (which typically do not go beyond $p = 3$), it is useful nonetheless to examine the performance of the proposed methodology in general applications where simultaneous prediction intervals are sought for large dimensions. The results, shown in Table 3.4, indicate that the proposed methodology still maintains accurate coverage even for $n = 50$. Moreover, the methodology of Lucagbo et al. (2022) performs well under multivariate normality but produces inaccurate coverage under the multivariate Cauchy setting.

Table 3.4: Estimated coverage probabilities (and their corresponding estimated standard errors expressed in parentheses) associated with the approaches to compute two-sided simultaneous prediction intervals using the (1) proposed methodology and (2) methodology of Lucagbo et al. (2022) when the dimension is large. The nominal level is set at 95%.

			Multivariate normal		Multivariate Cauchy	
n	Location Parameter	Scale Parameter	(1)	(2)	(1)	(2)
50	$\begin{bmatrix}0\\0\end{bmatrix}$	$\boldsymbol{\Sigma}_8$	0.9464 (0.0032)	0.9478 (0.0031)	0.9492 (0.0031)	0.9180 (0.0039)
200	$\begin{bmatrix}0\\0\end{bmatrix}$	$\boldsymbol{\Sigma}_8$	0.9484 (0.0031)	0.9502 0.0031	0.9534 (0.0030)	0.9606 (0.0028)

It is also of interest to check the performance of the proposed methodology when the assumption of symmetry does not hold. To this end, we implement the proposed methodology and that of Lucagbo et al. (2022) to the multivariate logistic distribution, which is a skewed distribution. Table 1.1 also shows its joint PDF. The estimated coverage probabilities and their associated standard errors are shown in Table 3.5. Interestingly, the proposed methodology still performs well, even when the sample size is relatively small. On the other hand, the benchmark methodology shows coverage probabilities below the nominal level.

Table 3.5: Estimated coverage probabilities (and their corresponding estimated standard errors expressed in parentheses) associated with the approaches to compute two-sided simultaneous prediction intervals using the (1) proposed methodology and (2) methodology of Lucagbo et al. (2022) for the multivariate logistic distribution. The nominal level is set at 95%.

p	n	Location Parameter	Scale Parameter	(1)	(2)
2	50	$\begin{bmatrix}0\\0\end{bmatrix}$	$[1 \quad 1]'$	0.9492 (0.0031)	0.9344 (0.0031)
			$[1 \quad 3]'$	0.9512 (0.0030)	0.9326 (0.0031)
	100	$\begin{bmatrix}0\\0\end{bmatrix}$	$[1 \quad 1]'$	0.9442 (0.0032)	0.9310 (0.0031)
			$[1 \quad 3]'$	0.9458 (0.0032)	0.9336 (0.0031)
	200	$\begin{bmatrix}0\\0\end{bmatrix}$	$[1 \quad 1]'$	0.9482 (0.0031)	0.9378 (0.0030)
			$[1 \quad 3]'$	0.9506 (0.0030)	0.9408 (0.0030)
3	50		$[1 \quad 1 \quad 1]'$	0.9482 (0.0031)	0.9350 (0.0031)

		$\begin{bmatrix}0\\0\\0\end{bmatrix}$	$[5 \quad 1 \quad 3]'$	0.9480 (0.0031)	0.9370 (0.0031)
	100	$\begin{bmatrix}0\\0\\0\end{bmatrix}$	$[1 \quad 1 \quad 1]'$	0.9472 (0.0032)	0.9294 (0.0033)
			$[5 \quad 1 \quad 3]'$	0.9476 (0.0032)	0.9284 (0.0033)
	200	$\begin{bmatrix}0\\0\\0\end{bmatrix}$	$[1 \quad 1 \quad 1]'$	0.9474 (0.0032)	0.9270 (0.0033)
			$[5 \quad 1 \quad 3]'$	0.9438 (0.0033)	0.9292 (0.0033)

Application: Laboratory Tests to Assess Liver Function

We now apply the proposed methodology to a dataset from Appendix 4.2 of Harris and Boyd (1995). The dataset includes the observed levels of two liver enzymes: alanine aminotransferase (ALT) and aspartate aminotransferase (AST) in U/L of 596 male medical students at the University of Virginia from 1987 to 1991. The goal is to construct an MRR for the analytes ALT and AST. Figure 1 shows the marginal density plots of ALT and AST. The plots indicate that both analytes are positively skewed. To satisfy the symmetry assumption, the data are first transformed using the Box-Cox transformation and then back-transformed to the original scale after applying the proposed procedure. The Box-Cox transformation parameters used are $\hat{\lambda}_1 = \hat{\lambda}_2 = -0.1414$. In Figure 2, we show the marginal density plots after the Box-Cox transformation. The density plots in Figure 2 indicate that the symmetry assumption is tenable for the transformed data, as opposed to the original data, where the assumption is clearly unwarranted. Table 3.6 shows the resulting two-sided simultaneous prediction intervals to be used as MRR. The prediction intervals for ALT and AST in Table 3.6 may be used as basis for reference intervals needed to diagnose liver function.

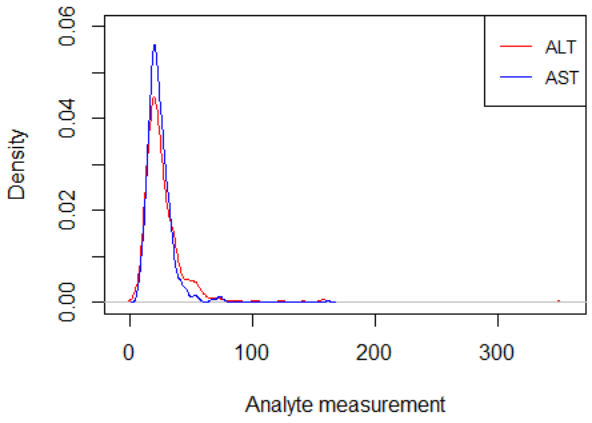

Figure 1: Marginal density plots of ALT (in U/L) and AST (in U/L)

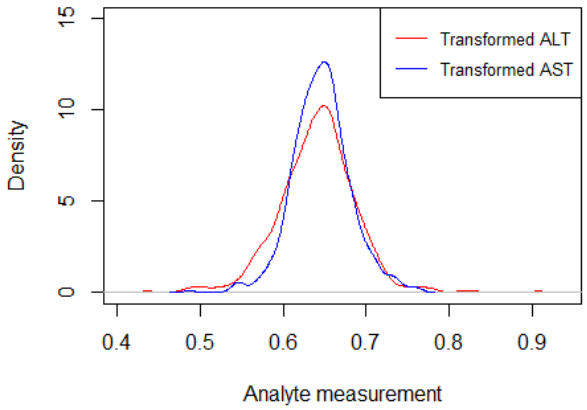

Figure 2: Marginal density plots of ALT and AST after transformation

Table 3.6: Multivariate reference region for ALT and AST computed using the proposed methodology to compute simultaneous prediction intervals

Analyte	Reference Limits
ALT	7.27 - 89.96
AST	9.28 - 59.57

CONCLUSION

Whenever there is a need to diagnose complicated conditions such as liver function or kidney function, it may not be sufficient to arrive at a diagnosis based on a single analyte. We have seen in Section 3.2 that liver function tests may include ALT and AST, as well as other common tests like alkaline phosphatase (ALP), albumin, and bilirubin. On the other hand, kidney function is diagnosed based on urea, uric acid, and creatinine. The use of combined univariate reference intervals for such cases is erroneous because it disregards the correlations among the analytes. As we have argued in this study, the correct approach is to use an MRR. While MRRs have been present in the laboratory medicine literature for decades, they have played a marginal role in actual laboratory medicine practice (Wellek 2011), largely due to difficulties with interpreting ellipsoidal reference regions. Harris and Boyd (1995, p.103) note that MRRs have largely remained "a statistical curiosity to the great majority of clinical chemists and clinicians and have little or no use in present-day clinical practice." In response to this problem, there has recently been active research in rectangular MRRs, beginning with the work of Wellek (2011). Other research works have followed suit, such as Young and Mathew (2020), Lucagbo et al. (2022), Lucagbo and Mathew (2023), and Liu et al. (2024).

In Section 1.1, we have mentioned the CLSI approved guideline for determining reference intervals, entitled *EP28-A3c: Defining, Establishing, and Verifying Reference Intervals in the Clinical Laboratory; Approved Guideline,* 3rd ed. The guideline has emphasized the use of robust methods in computing reference intervals. Referring specifically to the works of Horn (1988) and Kafadar (1982), the guideline states that "the working group would like to call attention to the 'robust method' because it may offer the best way of dealing with limited numbers of observations" (p. 1). The robust approach of Horn (1988) only applies to the univariate case, and no counterpart has been developed for the multivariate case. It seems that the development of a procedure that accounts for the correlations among the variables is a nontrivial problem. In this study, we have developed a methodology to compute a rectangular MRR that extends the robust biweight prediction interval of Horn (1988) to the multivariate case. This study devises a suitable bootstrap approach to estimate the prediction factor such that the correlations among analytes are properly accounted for, thereby obtaining robust simultaneous prediction intervals that may be used in computing the rectangular MRR. We emphasize that our study is not the first attempt at computing a rectangular prediction region, as past studies such as that of Lucagbo et al. (2022), have already proposed such regions. Neither is it the first time to introduce a rectangular MRR, since studies such as Wellek (2011) and Young and Mathew (2020) have constructed such MRRs albeit using different criteria. Instead, the main contribution of our study is the first attempt to compute a robust version of the rectangular

prediction region, which may then be used as an MRR. We also mention that the robustness claimed in this study is inherited from the robust univariate biweight estimator of location T_{bi}, and then the bootstrap is used to account for dependencies. We have not used a multivariate M-estimator of location, although there is robustness in the multivariate predictions. The proposed methodology shows accurate performance and clearly outperforms the benchmark methodology in all settings except when the underlying distribution is multivariate normal, in which case the two methodologies show similar performance. The proposed methodology yields consistent results even when the underlying distribution is heavy-tailed as it maintains coverage probabilities that are close to the nominal level. This indicates that the proposed methodology remains robust to the underlying data distribution and is resistant to the presence of outliers.

This study opens up a number of potential research topics. For example, it is certainly of interest to compute reference intervals and MRRs that depend on covariates such as a patient's age and sex. One future direction is to compute robust covariate-dependent MRRs. We hope to take this up in a future communication. Moreover, there has recently been a lot of research in MRRs that are computed using the criterion for tolerance regions. A notable property of reference regions computed through a tolerance region criterion is that they are amenable for multiple use. See the works of Young and Mathew (2020) and Lucagbo and Mathew (2023) for recent works on rectangular MRRs based on tolerance regions. In this regard, the computation of a rectangular MRR based on robust simultaneous tolerance intervals may also be explored in the future.

ACKNOWLEDGMENT

The authors are grateful to the anonymous reviewers for their valuable comments.

CONFLICT OF INTEREST

The authors report that there are no conflicts of interest to declare.

CONTRIBUTIONS OF INDIVIDUAL AUTHORS

Both authors contributed to the topic conceptualization, results generation, data analysis, and manuscript writing.

REFERENCES

Cambanis S, Huang S, and Simons G. On the theory of elliptically contoured distributions. Journal of Multivariate Analysis 1981; 11:368-385.

Clinical and Laboratory Standards Institute. EP28-A3c: Defining, Establishing, and Verifying Reference Intervals in the Clinical Laboratory; Approved Guideline (3rd ed.). Wayne, PA: CLSI, 2010.

Davison AC, and Hinkley DV. Bootstrap Methods and Their Application, Volume 1. Cambridge: Cambridge University Press, 1997.

Fang KT, Kotz S, Ng KW. Symmetric Multivariate and Related Distributions. Boca Raton, FL: Taylor & Francis Group, 1990.

Fisz M. Wahrscheinlichkeitsrechnung und mathematische Statistik. Berlin: VEB Deutscher Verlag der Wissenschaften, 1989.

Friendly M, Monette G, Fox J. Elliptical Insights: Understanding Statistical Methods through Elliptical Geometry. Institute of Mathematical Statistics 2013; 28(1):1-39.

Glivenko V. Giornale dell'Istituto Italiano degli Attuari 1933; 4: 92-99

Harris EK, Boyd, JC. Statistical Bases of Reference Values in Laboratory Medicine. New York, NY: Marcel Dekker, Inc, 1995.

Horn PS. A Biweight Prediction Interval for Random Samples. Journal of the American Statistical Association 1988; 83(401):249-256.

Horn PS, Pesce, AJ. Reference intervals: an update. Clinica Chimica Acta. 2003; 334:5-23.

Huber P. Robust Statistics. New York: John Wiley, 1981.

Ichihara K, Boyd JC. An Appraisal of Statistical Procedures Used in Derivation of Reference Intervals. Clinical Chemistry and Laboratory Medicine. 2010; 48(11):1537-1551.

Kafadar K. A Biweight Approach to the One-Sample Problem. Journal of the American Statistical Association. 1982; 77(378):416-424.

Kim B, Schulz J, Jung S. Kurtosis test of modality for rotationally symmetric distributions on hyperspheres. Journal of Multivariate Analysis. 2020; 178.

Liu RY. On a notion of simplicial depth. Proceedings of the National Academy of Sciences of the United States of America; 1981:1732-1734.

Liu W, Bretz F, Cortina-Borja M. Distribution-free hyperrectangular tolerance regions for setting multivariate reference regions in laboratory medicine. Statistics in Medicine. 2024; 43:1604-1614.

Lucagbo MD, Mathew T. Rectangular Tolerance Regions and Multivariate Normal Reference Regions in Laboratory Medicine. Biometrical Journal. 2023; 65.

Lucagbo MD, Mathew T, Young DS. Rectangular multivariate normal prediction regions for setting reference regions in laboratory medicine. Journal of Biopharmaceutical Statistics. 2022; 33(2):191-209.

Mosteller F and Tukey JW. Data Analysis and Regression: A Second Course in Statistics. Reading, Mass.: Addison-Wesley, 1977.

Rousseeuw PJ and Hubert M. Anomaly detection by robust statistics. WIREs Data Mining Knowl Discov. 2018; 8:e1236.

Wellek S. On easily interpretable multivariate reference region of rectangular shape. Biometrical Journal. 2011; 53(3):491-511.

Wilcox R. Introduction to Robust Estimation and Hypothesis Testing (3rd ed.). Oxford, UK: Elsevier Inc, 2012.

Young DS, Mathew T. Nonparametric hyperrectangular tolerance and prediction regions for setting multivariate reference regions in laboratory medicine. Statistical Methods in Medical Research. 2020; 29(12):3569-3585.